In: Advances in Medicine and Biology, Volume 15 ISBN: 978-1-61122-467-2
Editor: Leon V. Berhardt

Chapter 8

Mechanistic Insights into Prostanoid Transformations Catalyzed by Cytochrome P450. Prostacyclin and Thromboxane Biosyntheses

Tetsuya K. Yanai and Seiji Mori
Ibaraki University, Bunkyo, Mito, Japan

Abstract

Cytochrome P450s (P450) are an important class of proteins found in living organisms as they play a critical role in the metabolism of many endogenous and exogenous molecules. Examples of the former include the metabolites Prostacyclin (PGI_2) and thromboxane A_2 (TXA_2), which are biosynthesized from the substrate prostaglandin H_2 (PGH_2) by the P450s, prostalyclin and thromboxane synthases, respectively. Both metabolites play a key role in renal, cardiovascular, and pulmonary diseases so greater mechanistic understanding of the processes leading to their formation is highly desirable. Unlike typical cytochrome P450 reactions such as monooxygenations, synthases do not require O_2 or electron transfer from reductases for catalytic function. This is an area of active scientific interest in the area although there are several mechanistic proposals on the isomerization reactions of PGH_2, many aspects of the reaction still remain unclear. Recent research highlights include resonance Raman spectroscopic analyses that show the resting state of the thromboxane synthase bound with a substrate analogue contains a low-spin six coordinate heme. In addition, X-ray crystallographic studies on prostacyclin synthase indicate that the catalytic pocket is small and hydrophobic in character. Also worth mention are recent quantum mechanical (QM) studies that indicates homolytic O−O bond cleavage of PGH_2, is followed by one electron transfer from substrate to the heme, is essential for the generation of TXA_2 and PGI_2. In this chapter, we review the basic processes involved in heme and prostanoid chemistry and discuss the most recent studies in the area.

Introduction

TXA_2 and PGI_2 are arachidonic acid metabolites of considerable importance, the former being a potent mediator of platelet aggregation, vasoconstriction, and bronchoconstriction, and the latter a potent mediator of platelet anti-aggregation and vasodilation. [1, 2, 3,4]. In addition, these mediators have implications for diabetes mellitus and arrhythmia, and play a key role in cardiovascular and pulmonary diseases. [5, 6, 7]. Interestingly, PGI_2 and TXA_2 have opposing actions such as platelet aggregation and inhibition of platelet aggregation, respectively, although they are biosynthesized from the same substrate, PGH_2, and by same enzyme superfamily. TXA_2 and PGI_2 are formed from the same chemical precursor prostaglandin H_2 (PGH_2), in the former case being modified by the P450 as well as thromboxane synthase (TXAS), and in the latter case by the P450 prostacyclin synthase (PGIS). [8, 9] Scheme 1 and Figure 1)

A nonenzymatic hydrolysis step then leads to the conversion of TXA_2 into the more stable compound, thromboxane B_2 (TXB_2). TXB_2 is not the sole product of this reaction, with two other breakdown products namely, 12-L-hydroxy-5,8,10-heptadecatrienoic acid (HHT) and malondialdehyde (MDA) being produced in approximately equal amounts [10] dependent on the exact reaction condition [11]. PGI_2 is also converted into a more stable compound, 6-keto-prostaglandin $F_{1\alpha}$, by noneenzymatic hydrolysis.

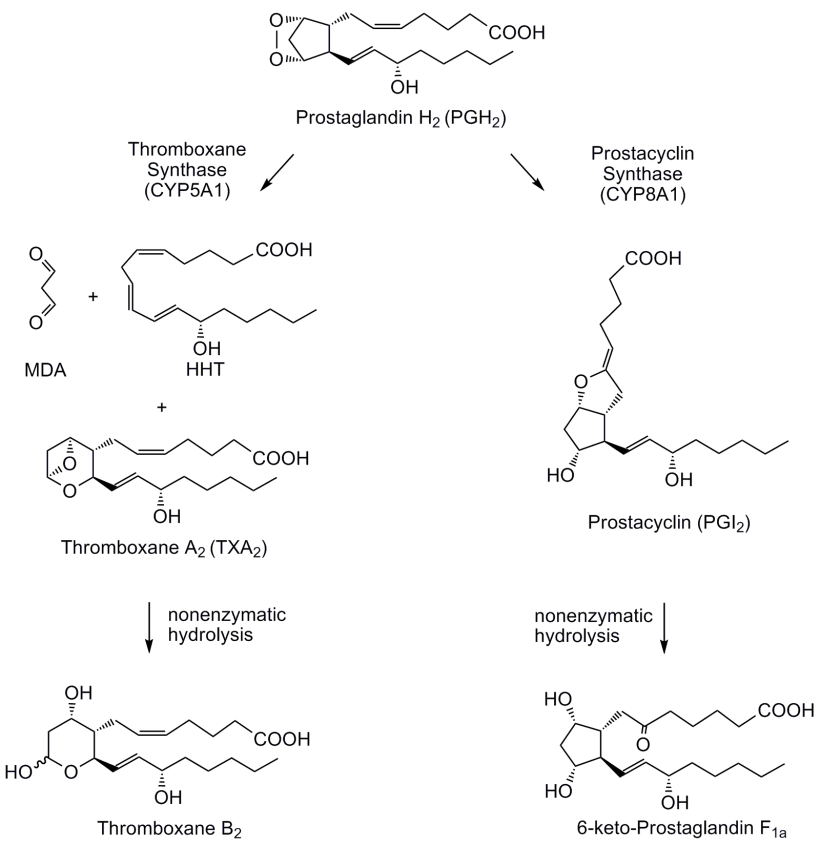

Scheme 1. Prostaglandin H_2 isomerizations to thromboxane A_2 and prostacyclin

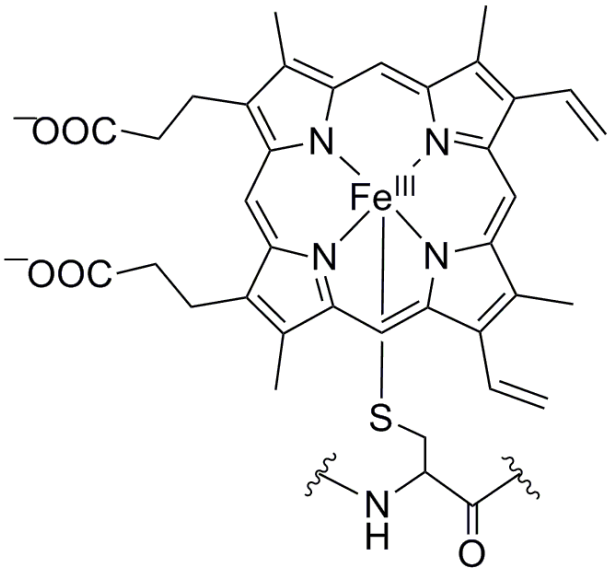

Figure 1. Heme-thiolate, Fe(III)-protoporphyrin IX with a cysteinate as an axial ligand, is an active center of cytochrome P450

Scheme 2. Monooxygenation by cytochrome P450

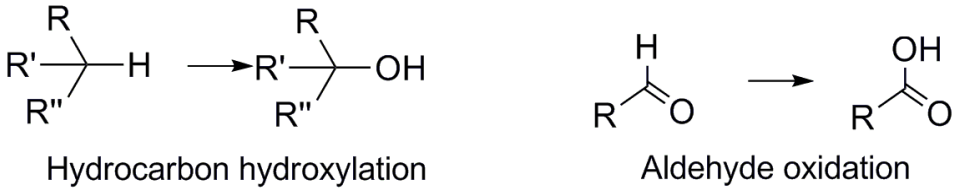

Scheme 3. Hydroxylation reactions catalyzed by cytochrome P450

The standard P450 catalytic cycle has been extensively studied by using spectroscopic [12] and theoretical approaches [13] and is shown in Scheme 4.

It is proposed that the Cytochrome P450 catalytic cycle starts from the resting hexacoordinate Fe^{III} complex (**1**) which has a water molecule as a distal ligand. ^{17}O electron spin-echo envelope modulation spectroscopy data for $P450_{CAM}$ shows that **1** has a doublet low-spin (LS) state. [14]. High-resolution optical and EPR spectroscopies at low temperature for $P450_{CAM}$ also show that the doublet ground state stays in spin equilibrium with a sextet high-spin (HS) state. [15, 16] Such a spin equilibrium can be observed in many kinds of cytochrome P450s [17, 18] using UV-vis spectra (HS and LS have ~390 and ~420 nm, respectively).

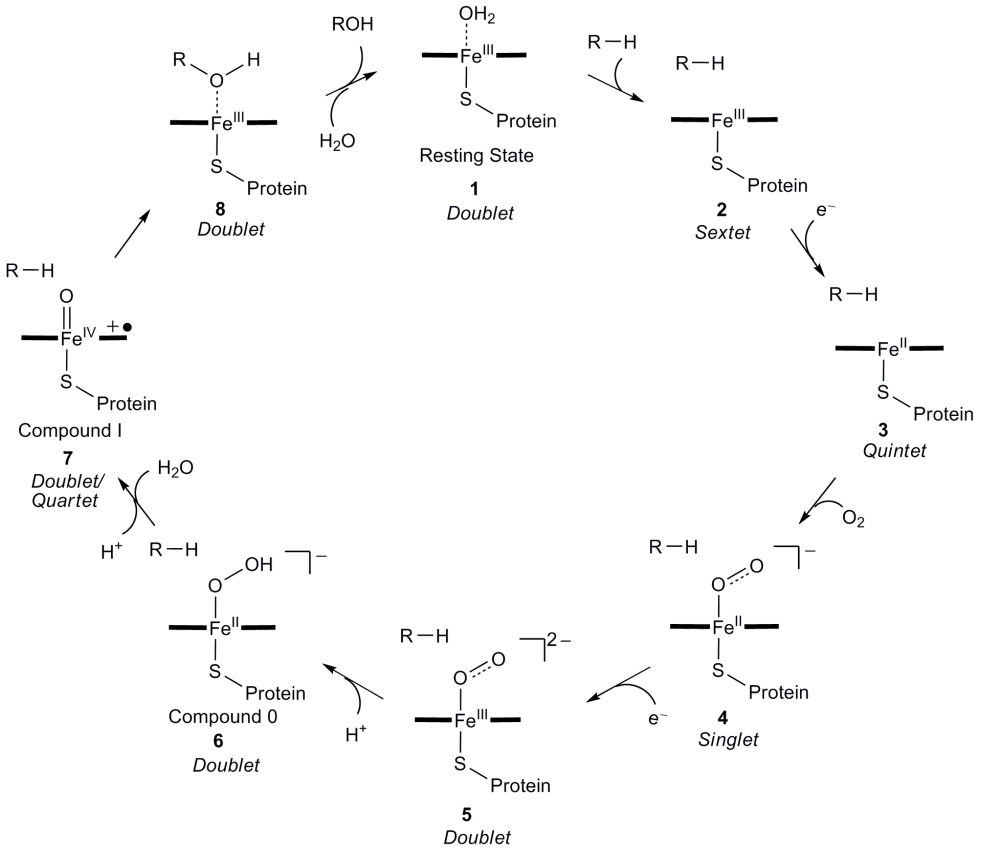

Scheme 4. Schematic representation of the catalytic cycle of cytochrome P450. R-H is a substrate. Spin states are texted in Italic

The spin equilibrium finding is also supported by quantum mechanics/molecular mechanics (QM/MM) calculations. [19]. A network of the water molecule occupy the active site pocket of the P450 and these must be displaced when a substrate binds into enzyme. [20]. This leads to the formation of a pentacoordinate Fe^{III} complex (**2**) with a sextet state] which is supported by QM/MM and density functional theory (DFT) calculations [21, 22, 23]. Substrate binding is also known to increase the redox potential of the protein following one electron reduction. [24]. The electron acceptor strength of the pentacoordinate complex (**2**) is higher than that of the resting state and, it can more easily accept an electron from a reductase, leading to a pentacoordinate Fe^{II} complex (**3**). The complex **3** has a high spin quintet state based on results from Mössbauer spectroscopy [25, 26] and DFT calculations [21, 23]. The formation of the pentacoordinate complex **3** then allows the binding by an O_2 molecule, leading to a hexacoordinate Fe^{II} peroxo complex (**4**). The some electron donation into the O-O π^* orbital of complex **4** has been observed by resonance Raman spectroscopy. [27, 28]. The electronic configuration of this complex is suggested to be a resonance structure of $Fe^{III}O_2^{-}$/ $Fe^{II}O_2$ based on the results of theoreticaland spectroscopicstudies. Subsequent reduction of **4** leads to a Fe^{III} peroxo complex (**5**). The distal peroxo in the complex **5** is sufficiently basic to be protonated by a water molecule or adjacent acidic residue leading to a Fe^{III} hydroperoxo complex (**6**), which is commonly referred to as "Compound 0". Kinetic

solvent isotope effect studies support this hypothesis that a water molecule is either directly or indirectly involved in the protonation step [29]. Compound 0, which has a high Lewis basicity, is protonated one more time. On protonation for a second time, the O–O bond cleaves, leading to a free water molecule and a high-valence Fe^{IV} oxo-complex (**7**), the so-called "Compound I". [30, 31] Theoretical studies suggest that the two steps involved in the formation of compound I proceed via doublet states [32, 33, 34].

Compound I is generally believed to be the active species in the cytochrome P450 catalytic cycle, although some suggest that Compound 0 can also be the active specis [35]. The chemical reactivity of compound I has been extensively studied but only indirect spectroscopic observation of this transient species has been reported [36, 37, 38, 39]. A P450 X-ray structure was initially reported to be that of compound I [40], however subsequent EPR and ENDOR experiments suggest that this was incorrect [36]. Given these difficulties, a large number of theoretical studies of P450s have been conducted to investigate this transient species. The majority of theoretical studies predict that Compound I has Fe^{IV} coordinated to a porphyrin π-cation radical [13].

The reactions catalyzed by compound I have been extensively studied in the literature. For example Groves and McClusky proposed a hydroxylation mechanism catalyzed by compound I which they term the "rebound mechanism" [41]. (Scheme 5) This mechanism proceeds through hydrogen abstraction, reorientation of the OH group, and rebound to form an alcohol molecule. It is suggested that the rate limiting step is either reduction of oxy-ferrous complex **4** or the subsequent protonation of Fe^{III} species **5** [42, 43]. More recently, experimental studies from Compound I that lead to the production of alcohols suggest that the activation energies for hydrocarbon oxidation are ~52-68 kJ/mol, considerably lower than the theoretical values [44]. In contrast, QM and QM/MM results of this mechanism show much lower activation energies at ~70-110 kJ/mol. [13, 45, 46, 47, 48]. Note that Friesner and coworkers predicted that the activation energy of the hydrogen abstraction for P450cam-catalyzed hydroxylation is 48.9 kJ/mol by B3LYP/MM calculations. [49]. Compound II, a Fe(IV)-oxo neutral porphyrin complex is proposed to be a short lived intermediate arising from compound I which has been characterized by UV-vis spectroscopy [50, 51] and XANES. [52]. In the final step, the monooxidized substrate described by complex (**8**) is displaced by a water molecule to complete the catalytic cycle of the cytochrome P450.

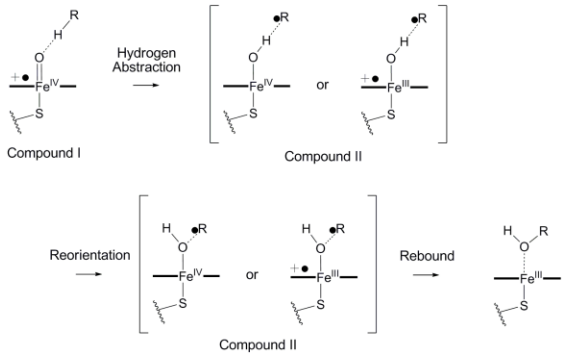

Scheme 5. A proposed mechanism for the compound I formation

Previously Proposed Reaction Mechanisms

The biosynthesis of TXA_2 and PGI_2, by TXAS and PGIS respectively, are classified as *isomerization reactions,* and are rather unusual among the cytochrome P450 catalyzed reactions. The mechanism leading to the formation of TXA_2 and PGI_2 are very similar due to the common substrate involved, which has lead to many mechanistic studies on both biosyntheses being conducted in parallel. As is the case for the standard P450 catalytic cycle, spin and electronic states of the reactive intermediates also remain unclear in the TXA_2/PGI_2 production.

Several reaction mechanisms associated with TXA_2/ PGI_2 formation have been proposed in the literature before information about TXAS and PGIS was known [53, 54, 55] on the basis of reactions of an endoperoxide with the Fe(II)-Fe(III) redox system (Scheme 6), [56, 57, 58] Diczfalusy et al. subsequently incubated [1-^{14}C]PGH_2 with purified TXAS from human platelet and proposed a mechanism involving heterolytic endoperoxide O−O bond cleavage induced by protonation (Scheme 7) [59, 60]. They also showed that the breakdown products of PGH_2, MDA and HHT were not formed alongside TXA_2. Fried and Barton proposed mechanisms of TXA_2 and PGI_2 formations initiated by heterolytic O−O bond cleavage (Scheme 8). [61].

In the 1980s, Ullrich and co-workers concluded that TXAS and PGIS were responsible for TXAS and PGIS formation with the aid of EPR and optical spectroscopic analyses. They also determined that both proteins belonged to the cytochrome P450 superfamily [62, 63] (Table 1) They found that reduction of both TXAS and PGIS by sodium dithiolate in the presence of CO shifted the Soret maxima at 418 and 417 to 450 and 451 nm, respectively. The red-shifted peaks at ~450 nm are typical as well as EPR spectra data confirmed the proteins were members of the P450 superfamily. The fact that these spectra are similar to that of hexa-coordinate P450, having a water molecule as the axial ligand, [64] suggests that the resting TXAS and PGIS structures correspond to aqua-coordinated low spin Fe complexes.

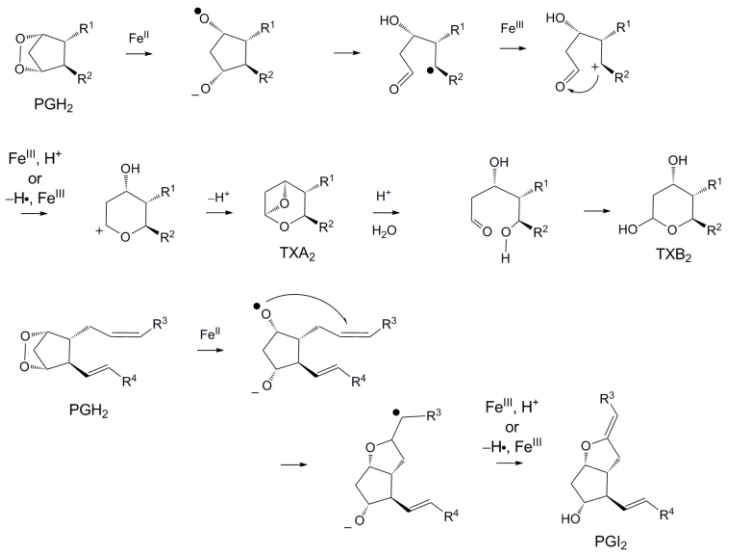

Scheme 6. Previously proposed Fe(II)-induced reaction mechanisms of TXA_2 and PGI_2 biosyntheses

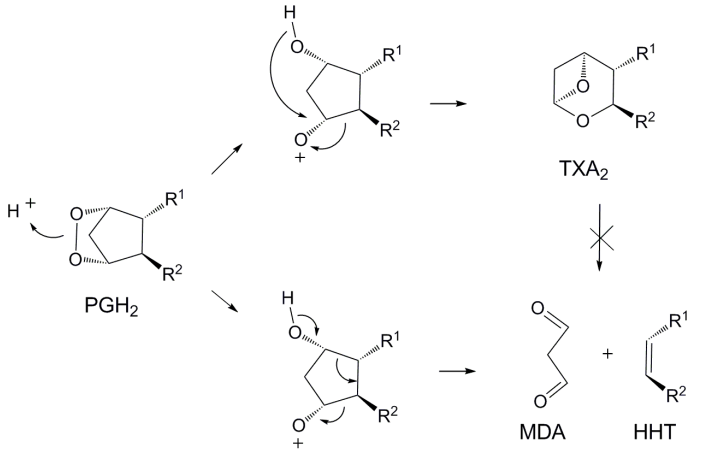

Scheme 7. Previously proposed reaction mechanism of TXA_2 involving heterolytic endoperoxide O-O bond cleavage

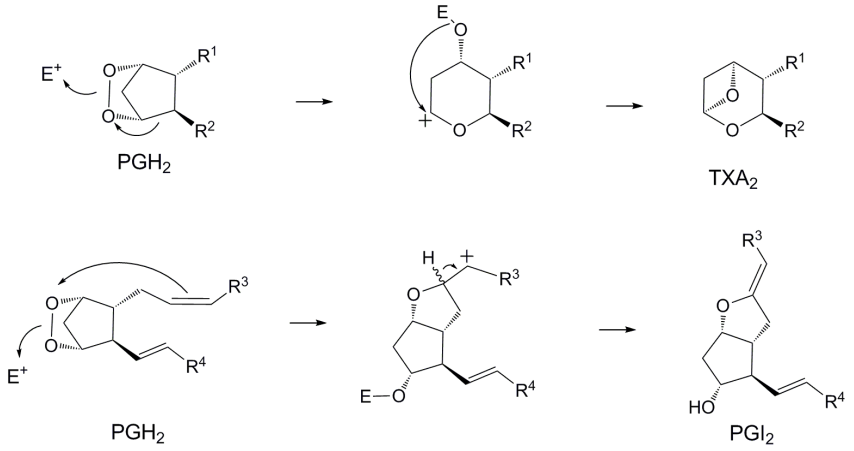

Scheme 8. Previously proposed reaction mechanism of PGI_2 involving heterolytic endoperoxide O-O bond cleavage

Table 1. Spectral properties of resting TXAS and PGIS. Data are taken from references of 63**, 64, and a review 66**

	TXAS	PGIS	$P450_{CAM}$
g-value (oxidized)	2.41, 2.25, 1.92	2.42, 2.25, 1.92	2.45, 2.26, 1.91
abs [nm] (oxidized)	418, 537, 570	417, 532, 568	417, 536, 569
abs [nm] (reduced + CO)	424, 450, 545	424, 451, 545	

In 1989, the reaction mechanisms for TXA_2 and PGI_2 biosynthesis were proposed by Hecker and Ullrich based on experiments with isotope labeled PGH_2 and analogues (Scheme 9 and 10) [65]. In the case of TXA_2 biosynthesis, the endoperoxide oxygen atom at C(9) must

attach to the heme iron(III) of TXAS (**i**). The mechanism proceeds with the homolytic cleavage of the PGH_2 endoperoxide O−O bond, resulting in a hexacoordinate Fe^{IV}-porphyrin intermediate (**ii**) with an alkoxy radical. This is followed by β-scission of the alkoxy radical yielding products with a carbon-centered radical (**iii**). Finally, the substrate forms a zwitterion (**iv**) by one electron transfer from the carbon-centered radical to the heme-iron to give TXA_2, or alternatively, decomposes into HHT and MDA.

The mechanism of PGI_2 biosynthesis is similar to that of TXA_2 as previously discussed (Scheme 10). In the first step, the endoperoxide oxygen atom at C(11) attaches to the heme iron of PGIS (**i**). Next, the mechanism proceeds with the homolytic cleavage of the PGH_2 endoperoxide O−O bond, which results in a hexacoordinate Fe^{IV}-porphyrin intermediate with an alkoxy radical (**ii**), followed by C–O bond formation that yields a carbon radical complex (**iii**). Finally, a substrate forms a zwitterion (**iv**) to give PGI_2 by the elimination of a C(6)-proton.

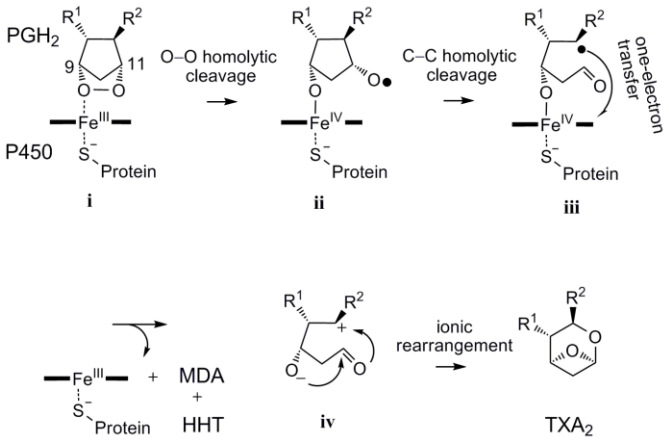

Scheme 9. Previously proposed reaction mechanism of TXA_2 biosynthesis. (R^1: $CH_2CH{=}CHC_2H_6COOH$, R^2: $CH{=}CHCH(OH)C_5H_{11}$)

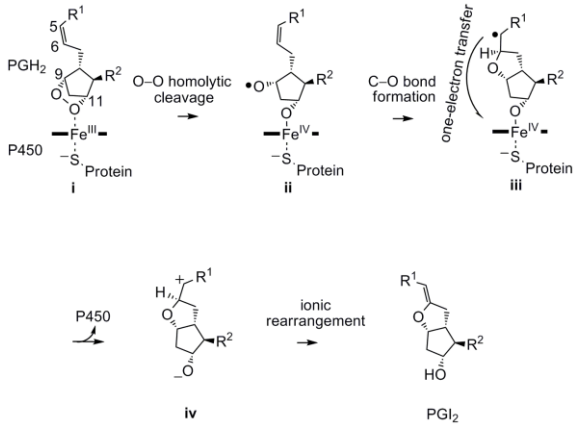

Scheme 10. Previously proposed mechanism of prostacyclin biosynthesis. (R^1 : C_3H_6COOH, R^2 : $CH{=}CHCHOHC_5H_{11}$)

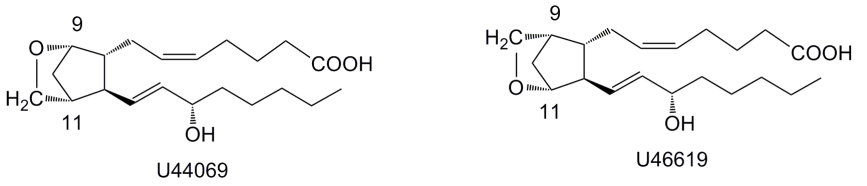

Figure 2. Structures of U44069 and U46619

Table 2. Biomimetic PGH_2 conversion. Data are taken from ref. 67. PPIXDME : protoporphyrin IX dimethyl ester. hemin : ferric protoporphyrin IX. Structures of PPIXDME and hemin are illustrated in Figure 3

Test sytem	Product formation						
	6-keto-$PGF_{1\alpha}$	TXB_2	$PGF_{2\alpha}$	PGE_2	PGD_2	HHT	Others
%							
Buffer			0.8	88.9	5.8	0.8	3.7
$FeCl_2$/buffer	-	-	1.4	59.1	11.2	6.9	21.4
$FeCl_2/CH_3CN$	-	-	0.7	19.7	4.4	14.1	61.1
$FeSO_4$/buffer	-	-	0.8	8.2	2.3	25.8	62.9
Hemin/buffer	0.5	0.5	2.4	51.6	11.8	9.3	23.9
$Hemin/CH_3CN$	1.0	0.8	1.0	28.5	6.6	32.8	29.3
PPIXDME-S^- /CH_2Cl_2	1.2	0.6	0.3	9.9	4.3	36.0	47.7
PPIXDME-Cl^- /CH_2Cl_2	0.5	1.0	2.4	5.9	7.5	23.2	59.5

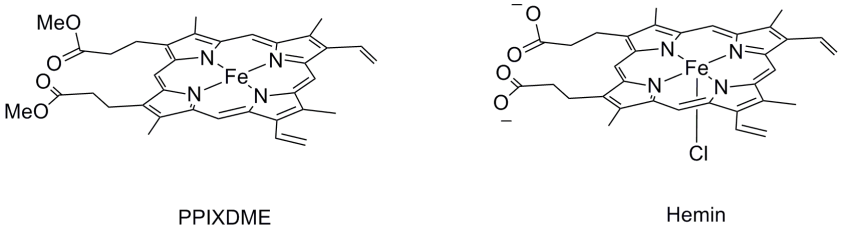

Figure 3. Structures of PPIXDME (protoporphyrin IX dimethyl ester) and hemin (ferric protoporphyrin IX)

In TXA_2/ PGI_2 biosyntheses, it is not clear which endoperoxide oxygen atom binds to the heme iron. The ligand binding mode to heme iron in both TXAS and PGIS were suggested from optical difference spectra using inhibitors, 9,11-epoxymethano-$PGF_{2\alpha}$ (U44069) and 11,9-epoxymethano-$PGF_{2\alpha}$ (U46619). (Figure 2) In case of TXAS with U44069, a ligand-type (i.e 6-coordinate) spectrum was observed, whereas with U46619 bound with TXAS an unbound, five-coordinate-type spectrum was found [65]. Interestingly, the trends were reversed for PGIS. More recently, resonance Raman spectroscopic analyses on U46619 binding to TXAS have shown the possibility that the oxygen atom at C(11) binds to heme iron, in contradiction to the optical difference spectroscopic studies. [66]. These suggest that

both the O(9) and O(11) atoms can coordinate TXAS. Further studies are necessary to distinguish the endoperoxide oxygen binding of TXAS for the real substrate, PGH_2 rather than analogs.

It is proposed that TXA_2/PGI_2 biosynthesis occur from an Fe^{III}-porphyrin complex. This is based on the findings of Hecker and Ullrich who demonstrated that the formation of TXA_2 and PGI_2 is only catalyzed by Fe^{III}-porphyrin catalysts: Hemin, PPIXDME-S^-, and PPIXDME-Cl^-. (Table 2 and Figure 3) Spectroscopic investigation of the spin state of the TXAS-PGH_2 complex was subsequently performed by Wang and co-workers using a recombinant TXAS-U44069 protein complex as a mimic of the TXAS-PGH_2 [67]. The resultant absorption spectra peaks at (414, 531.5 & 563 nm) [67] are characterized as being a typical oxygen donor-coordinated ferric low-spin P450 complex akin to the $P450_{CAM}$ complex which displays peaks at: 416~420, 533~539, 566~571 nm. [68]. Magnetic circular dichroism (MCD) spectra also showed Soret crossover and peaks of typical low-spin P450. Moreover, electron paramagnetic resonance (EPR) investigations, one of the most useful approaches for assignment of spin state, measured a *g*-value of 2.484, 2.252, and 1.900, showing the hexa-coordinate ferric complex was low-spin (S = 1/2). This compares with several hexa-coordinate $P450_{CAM}$ structures having oxygen-based axial ligand have EPR g-values of 2.43~2.48, 2.25~2.27, and 1.91~1.93. (Note that in camphor-bound P450cam, the EPR g-values are 3.95, 7.80, and 1.78. [69]) In addition to the EPR and MCD spectra, resonance Raman spectra has provided the same conclusion. [59]/.

Comparable results were reported in PGIS by Wang and co-workers using a recombinant PGIS-U46619 complex [70]. Absorption, MCD, and EPR spectra indicate that the U46619 complex corresponds to a hexa-coordinate ferric low-spin P450 structure. The results also suggest that the starting complexes, TXAS-PGH_2 and PGIS-PGH_2 must have a hexa-coordinate ferric low-spin heme.

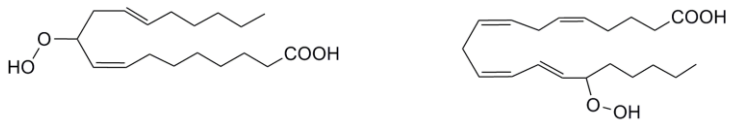

Figure 4. Lipid hydroperoxides, 10-hydroperoxyoctadeca-8,12-dienoic acid and 15-hydroperoxyeicosatraenoic acid

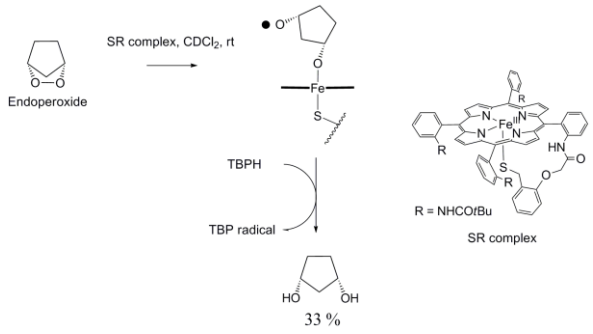

Scheme 11. Radical trapping of alkoxyradical by TBPH

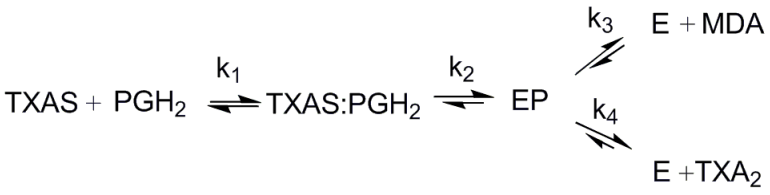

Scheme 12. PGH_2 transformation catalyzed by TXAS. EP refers an intermediate

Table 3. Rate constants for kinetic simulation of TXAS

Explt.	$k_1 \times 10^{-6}$	k_1	k_2[a]	k_3[a]	k_4[a]
	$M^{-1}s^{-1}$	s^{-1}	s^{-1}	s^{-1}	
5 μM PGH_2	12	360	15,000	6,000	4,000
15 μM PGH_2	20	360	15,000	6,000	4,000
50 μM PGH_2	12	360	15,000	6,000	4,000

[a] The numerical values are set to be 0.01.

Experimental kinetic data for the TXA_2 and PGI_2 biosyntheses provide us with valuable information on the reaction mechanism. For example, Hecker and Ullrich suggested that the rate limiting step for TXA_2 and PGI_2 formation is not the O-O bond cleavage step. This was based primarily on the basis of a lack of primary hydrogen kinetic isotope effect when deuterated PGH_2 was used [65]. The kinetics for PGH_2 and its analogues U44069 (Figure 2) with TXAS suggest that the rate-limiting step for TXA_2 biosynthesis is not the isomerization process but the substrate-binding step into TXAS [71]. The authors also simulated rate constants for the isomerization step based on the kinetic experiments.(Scheme 12, Table 3) The calculated rate constant k_2, of 15,000 s^{-1} suggests that the chemical reaction is extremely fast. However, the kinetics associated with the isomerization step of PGI_2 biosynthesis have not been reported.

Structural Information of PGIS

The known amino acid sequences of bovine, [72, 73] human, [74], rat, [75], mouse, [76] and zebrafish [77]. PGISs have been used to guide site-directed mutagenesis studies of human PGIS [78, 79] until X-ray crystal structures are available. These results indicate that Ile67, Val76, Pro355, Glu360, Asp364, and Leu384 residues are essential for catalytic activity.

Recently, the group of Chan and Wang's succeeded in their efforts to obtain an X-ray structure of human PGIS (Figure 5) [80]. In the resting state structure, Cys441 is connected to Gly443 and Arg444 by two inter-molecular H-bonds. Note that some residues such as Ile67, Glu360, Asp364, and Leu385 demonstrating the important catalytic activity [79] do not exist in the active site. A docking study of PGH_2 into the active site suggested that that the binding pocket of human PGIS is relatively small compared with that of other cytochrome

P450s, and also suggested that Trp282, which lies towards the top of the active site cavity, forces the PGH_2 side chains to adopt an outstretched binding conformation. This outstretched binding conformation has also been proposed by Ullrich and Brugger [80]. In contrast, high-resolution NMR spectroscopic and docking studies of U46619 with PGIS suggested that two side chains of PGH_2 are compacted on substrate binding due to the narrower PGIS active site. [81]. Subsequently, the X-ray crystal structures of the resting state of human PGIS, (a) minoxidil-bound human PGIS, (b) ligand-free zebrafish PGIS, and (c) U51605-bound zebrafish PGIS, were reported by the group of Chan and Wang [72]. These structures showed that heme moiety changes its position on the direct Fe binding of the inhibitor minoxidil. Both the human and zebrafish PGIS showed the same trend (Figure 6).

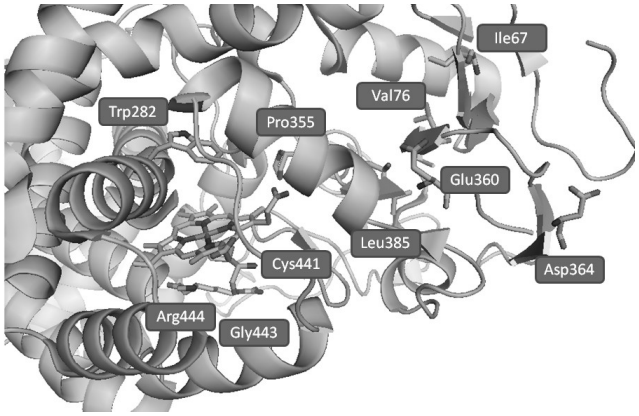

Figure 5. Active site of human PGIS (PDB ID: 2IAG [84])

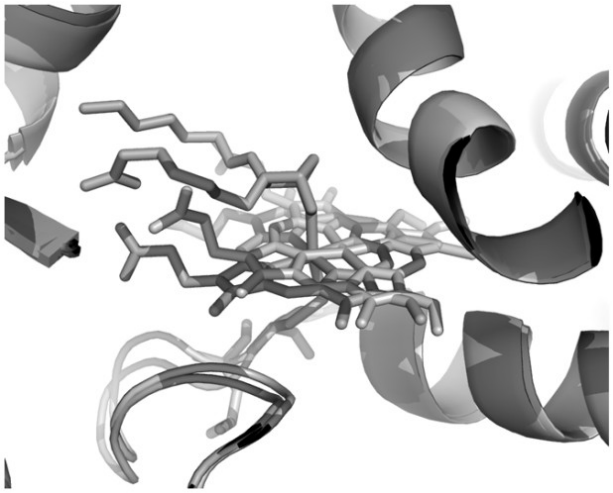

Figure 6. Superimposed structure for U51605-free and U51605-bound zebrafish PGIS (PDB ID: 3B98 and 3B99)

Structural Information of TXAS

Although an X-ray crystal structure of TXAS is not yet available, a number of mutagenesis studies and homology modeling exercises have been published. A schematic representation of the predicted model of human TXAS is shown in Figure 7. The amino acid sequences of human, [82, 83, 84] rat, [85] murine [86], porcine [87]. TXASs have been established. Ruan and co-workers used homology modelling to generate a 3-D model for TXAS using $P450_{CAM}$ and $P450_{BM3}$ as templates (26.4% residue identity and 48.4% residue similarity). The results helped to elucidate characteristics of the substrate binding pocket and allowed docking studies of PGH_2 to be performed [88]. Subsequent mutagenesis studis [92, 89] showed that Ala408, Arg413, Asn110, Phe127, Arg478, and Cys480 are essential for catalytic activity [90]. The following insights were suggested: Ala408 is essential for creation of the hydrophobic substrate binding pocket, interacting with hydrophobic region of PGH_2. The dissociation constants of imidazole-based, pyridine-based, and pyrimidine-based ligands with recombinant TXAS confirm that the active site is hydrophobic in nature and larger than typical cytochrome P450s [64]. Arg413 interacts with the carboxylate group of PGH_2 while Asn110, Phe127, and Arg478 are critical for binding the heme moiety.

Additional Mutagenesis and EPR studies [91] on TXAS have shown that the propionates groups of the heme form a number of H-bonds with active site residues including: Asn110, Arg413, Arg478, Trp133, and Arg137 through direct or indirect hydrogen bonds. In addition to these mutagenesis studies, resonance Raman spectra on a resting state, recombinant TXAS-PGH_2 analogue complexes (U44069 and U46619, see Figure 2) have given us additional structural information [66].

The resultant spectra indicated that the vinyl groups of heme in the resting TXAS complex assume an in-plane conformation and that substrate binding causes displacement of one of the vinyl groups. Additionally, a strong hydrogen-bond between 6-propionate group and Arg137 is disrupted upon binding of U44069 [66]. These suggestions are supported by the earlier mutagenesis study [89]. Furthermore, comparison of Fe-S vibration of TXAS with that of other heme thiolate enzymes, typical P450, chloroperoxidase, and nitric oxide synthase, indicated that the proximal thiolate group has two hydrogen bonds with peptide NH groups.

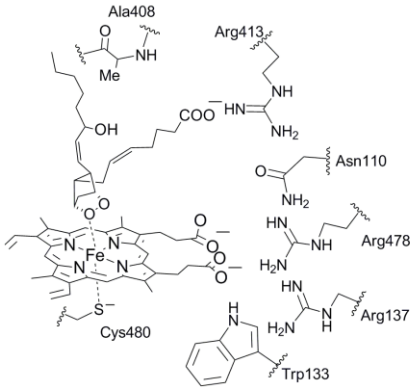

Figure 7. A Schematic representation of predicted human TXAS active site bound by PGH_2. Residues required for catalytic activity are shown

Recently Proposed TXAS Mechanism

Although many approaches to elucidate the aspects of reactivity and structure have been proposed, experimental constraints make it difficult to study the isomerization process, especially the oxidation state of Fe over the course of the reaction. Most recently, Yanai and Mori investigated the mechanisms of PGH_2 isomerization cytochrome P450 model using the symmetry-broken unrestricted Becke-three-parameter plus Lee–Yang–Parr (UB3LYP) DFT method [92, 93]. They proposed a new reaction mechanisms for TXA_2 [94] and PGI_2 [95] biosyntheses on the basis of their theoretical results and the previously experiment results as shown in (Scheme 13 and 14)

The first step in TXA_2 mechanism sees the endoperoxide oxygen atom at the C(9)-position of PGH_2 attach to the heme iron bound in the TXAS active site. Next, an alkoxy radical intermediate is formed by O–O hemolytic bond cleavage, followed by the formation of an allyl radical intermediate (compound II), with C(11)–C(12) bond cleavage of the alkoxy radical intermediate. Finally, the formation of a 6-membered ring in conjunction with one electron transfer leads to the production of TXA_2. The homolytic cleavage of C(8)–C(9) bond competitively leads to fragmentation products (HHT and MDA). This mechanism differs from the previous one by Ullrich, et al with respect to the one electron transfer step that leads to the six-membered ring formation. The theoretical results also show that the one electron transfer to the heme iron from the allyl group in the oxanyl ring formation step is essential to facilitate TXA_2 formation. Moreover, two possible reaction pathways through the Fe^{IV} intermediates or Fe^{III}-porphyrin π-cation radical intermediates are suggested by the theoretical results, although the later one is a minor pathway. The rate limiting step following PGH_2 binding to TXAS is the homolytic cleavage of the O–O bond in PGH_2 as suggested by Hecker and Ullrich [65]. The TXA_2 formation should proceed spontaneously with a homolytic O−O bond cleavage since the overall reaction is exothermic and has lower activation barriers of ~52.5 kJ/mol. This compares to theoretically estimated activation energies of typical cytochrome P450-catalyzed reactions, hydroxylation, are ~70-110 kJ/mol [13]. The lower activation barrier associated with TXA_2 is consistent with previous kinetics studies [72].

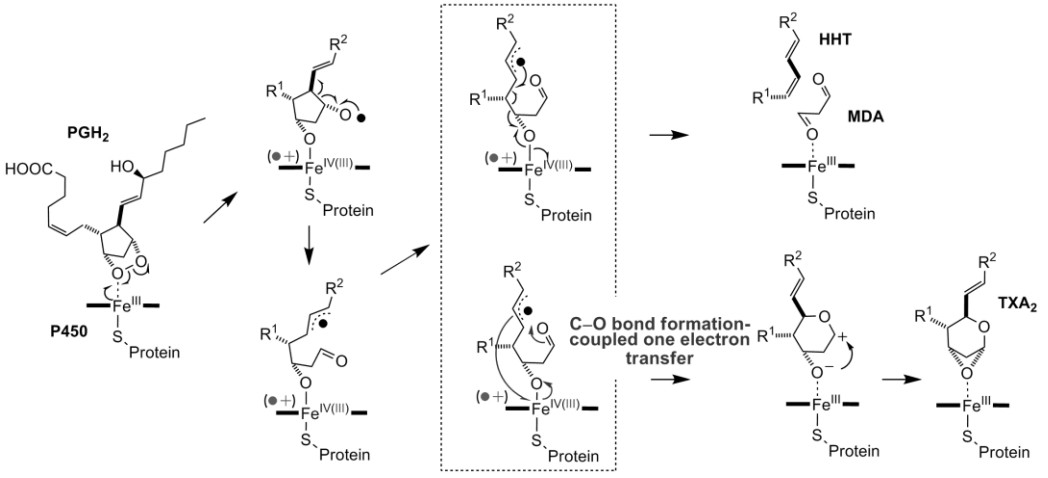

Scheme 13. Newly proposed reaction mechanism of thromboxane A_2 (TXA_2) biosynthesis

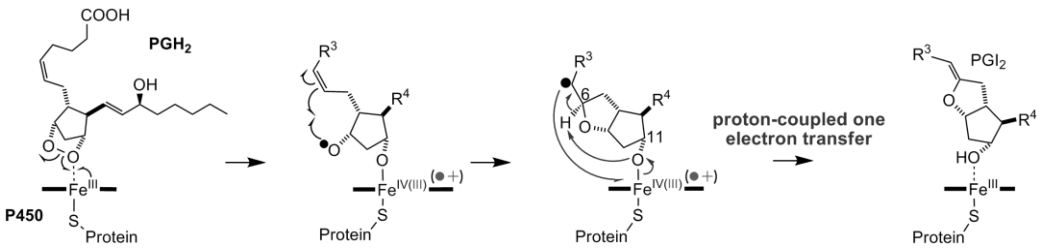

Scheme 14. Newly proposed reaction mechanism of prostacyclin (PGI_2) biosynthesis

Recently Proposed PGIS Mechanism

The proposed reaction mechanism for PGI_2 biosynthesis is similar to that for TXA_2. First, the endoperoxide oxygen atom at C(11) attaches to the heme iron of PGIS. Next, the mechanism proceeds with the homolytic cleavage of the PGH_2 endoperoxide O−O bond, which results in a hexacoordinate intermediate with an alkoxy radical (compound II). This is followed by C−O bond formation that yields products with a carbon radical complex. Docking simulations of PGIS with PGH_2 based on the resting state X-ray crystal structure predicted that the C(6) atom lies near the O atom at C(9) position. The docking simulations are supported by high-resolution NMR spectroscopic studies on structure of PGH_2 analogue (U46619) binding to PGIS [81]. Finally, a substrate forms zwitterion to give PGI_2 by the elimination of a C(6)-proton. The density functional mechanistic investigation of PGI_2 biosynthesis also revealed that the rate-limiting step for the reaction of endoperoxide with Fe^{III}-porphyrin is the O–O bond homolytic cleavage as is the case for TXA_2 [95]. The activation energy for the PGI_2 process is ~45 kJ/mol, also lower than other that of classical P450-catalyzed reaction. The theoretical studies also showed that the PGH_2 isomerization into PGI_2 by atypical P450 enzyme proceeds through proton coupled electron transfer (PCET) [96] to give a PGI_2-PGIS complex with low activation energy. The doublet electronic configuration of heme moiety in the PGI_2 mediated process is similar to that in the TXA_2, and is consistent with the previous experimental results [70]. Additionally, theoretical studies on an extended model including an important active site residues Trp282 [95]based on the X-ray crystal structure of zebrafish PGIS, also showed that the isomerization proceeds in the doublet low-spin state which is consistent with earlier experimental studies. [66, 67]

An interesting observation from recent experimental and theoretical studies described herein is that both biosyntheses proceed through a process involving one-electron transfer coupled with proton transfer and C–O bond formation. This mechanism is novel in P450 catalysis and evidence for its existence comes from recent theoretical studies of C-C bond formation of chromopyrrolic acid with P450 StaP (CYP245A1) (Figure 8). [96, 97].

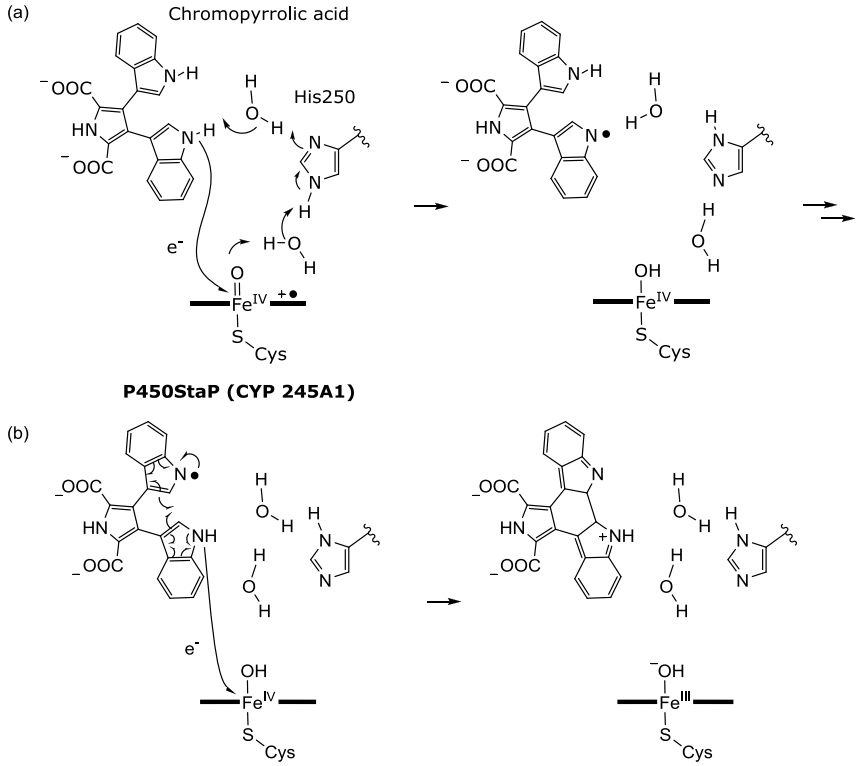

Figure 8. (a) Proton-coupled electron transfer and (b) C-C bond formation coupled electron transfer processes in P450StaP-catalyzed reaction. The mechanism is taken from ref. and modified.

Conclusion

The isomerization processes associated with $PGH_2$are unusual from a cytochrome P450 perspective, so their investigation is important to shed light on this relatively under-studied subject. Presented herein is a review of recent studies on the mechanism of TXA_2 and PGI_2 formations catalyzed by cytochrome P450, which has been compared and contrasted with typical reaction mechanisms catalyzed by cytochrome P450 and those of prostaglandin chemistry and biochemistry. The radical mechanism initiated by homolytic O-O bond cleavage and one-electron transfer from substrate to Fe is essential to such a kind of transformation.

Our understanding of TXA_2 and PGI_2 biosyntheses has increased dramatically over the past few years as result of many biochemical, biomimetic, and theoretical studies reported in the literature. As a result of this research work we have obtained considerable mechanistic insight into this important, catalytically driven process and it is expected that this trend will continue given the amount of research in this important area of science. From the considerable amount of literature on the subject we can conclude the TXA_2 and PGI_2 biosynthetic mechanisms, which involves radical mechanism starting from homolytic O-O bond cleavage, can be compared with other prostanoid biosyntheses from PGH_2 to PGD_2 or PGE_2, which are assumed to be transformed through nucleophilic/base mechanism with deprotonated glutathione [98, 99, 100, 101].

Acknowledgment

We are grateful for Dr. M. Paul Gleeson, Kasetsart University, Thailand, for his careful reading of the manuscript and valuable comments. This work was supported by Grants-in-Aid for Scientific Research No. 19550004 from JSPS and by Scientific Research on Priority Areas "Molecular Theory for Real Systems", No. 20038005, from MEXT. The generous allotment of computational time from the Research Center for Computational Science (RCCS), the National Institutes of Natural Sciences, Japan, is also gratefully acknowledged.

References

[1] Ogletree, M. L. (1987). Overview of physiological and pathophysiological effects of thromboxane A_2. *Fed. Proc*., *46*, 133–138.

[2] Ullrich, V. & Zou, M.-H. (2001). Bachschmid, M. New physiological and pathophysiological aspects on the thromboxane A_2-prostacyclin regulatory system. *Biochim. Biophys. Acta Mol. Cell Biol. Lipids, 1532*, 1–14.

[3] Moncada, S. & Vane, J. R. (1978). Pharmacology and endogenous roles of prostaglandin endoperoxides, thromboxane A_2, and prostacyclin. *Pharmacol. Rev., 30*, 293–331.

[4] Vane, J. R. & Bonting, R. M. (1995). Pharmacodynamic profile of prostacyclin. *Am. J. Cardiol*, *75*, 3A–10A.

[5] Halushka, P. V., Rogers, R. C., Loadholt, C. B. & Colwell, J. A. (1981). Increased platelet thromboxane synthesis in diabetes mellitus. *J. Lab. Clin. Med., 97*, 87–96.

[6] Coker, S. J., Parratt, J. R., Ledingham, I. M. & Zeitlin, I. J. (1981). Thromboxane and prostacyclin release from ischaemic myocardium in relation to arrhythmias. *Nature, 291*, 323–324.

[7] Mehta, J. L., Lawson, D., Mehta, P. & Saldeen, T. (1988). Increased prostacyclin and thromboxane A_2 biosynthesis in atherosclerosis. *Proc. Natl. Acad. Sci. USA*, *85*, 4511–4515.

[8] Ullrich, V. & Graf, H. (1984). Prostacyclin and thromboxane synthase as P-450 enzymes. *Trends Pharmacol. Sci.*, *5*, 352–355.

[9] Needleman, P., Turk, J., Jakschik, B. A., Morison, A. R. & Lefkowith, J. B. (1986). Arachidonic acid metabolism. *Annu. Rev. Biochem.*, *55*, 69–102.

[10] Hammarström, S. & Falardeau, P. (1977). Resolution of prostaglandin endoperoxide synthase and thromboxane synthase of human platelets. *Proc. Natl. Acad. Sci. USA*, *74*, 3691–3695.

[11] Shen, R.-F. & Tai, H.-H. (1986). Immunoaffinity purification and characterization of thromboxane synthase from porcine lung. *J. Biol. Chem.*, *261*, 11592–11599.

[12] Ortiz de Montellano, P.R. (1986). Cytochrome P-450: Structum, Mechanism and Biochemistry, Plenum Press, New York.

[13] Denisov, I. G., Makris, T. M., Sligar, S. G. & Schlichting, I. (2005). Structure and chemistry of cytochrome P450. *Chem. Rev*., *105*, 2253-2278.

[14] Shaik, S., Kumar, S., de Visser, S. P., Altun, A. & Thiel, W. (2005). Theoretical perspective on the structure and mechanism of cytochrome P450 enzymes. *Chem. Rev*., *105*, 2279–2328.

[15] Thomann, H., Bernardo, M., Goldfarb, Kroneck, P. M. H. & Ullrich., V. (1995). Evidence for water binding to the Fe center in cytochrome P450cam obtained by ^{17}O electron spin-echo envelope modulation spectroscopy. *J. Am. Chem. Soc.***,** *117*, 8243–8251.

[16] Sligar, S. G. (1976). Coupling of spin, substrate, and redox equilibriums in cytochrome P450. *Biochemistry*, *15*, 5399–5406.

[17] Tsai, R., Yu, C. A., Gunsalus, I. C., Peisach, J., Blumberg, W., Orme-Johnson, W. H. & Beinert, H. (1970). Spin-state changes in cytochrome P-450_{cam} on binding of specific substrates. *Proc. Natl. Acad. Sci. USA*, *66*, 1157–1163.

[18] Roberts, A. G., Campbell, A. P. & Atkins, W. M. (2005). The Thermodynamic Landscape of Testosterone Binding to Cytochrome P450 3A4: Ligand Binding and Spin State Equilibria, *Biochemistry***,** *44,* 1353-1366. References cited therein.

[19] Kirsty J. McLean, K. J., Warman, A. J., Seward, H. E., Marshall, K. R., Girvan, H. M., Cheesman, M. R., Waterman, M. R. & Munro, A. W. (2006). Biophysical Characterization of the Sterol Demethylase P450 from *Mycobacterium tuberculosis*, Its Cognate Ferredoxin, and Their Interactions, *Biochemistry, 45,* 8427-8443.

[20] Schöneboom, J. C. & Thiel, W. (2004). The resting state of $P450_{cam}$: A QM/MM study. *J. Phys. Chem. B*, *108*, 7468–7478.

[21] Di Primo, C., Hui Bon Hoa, G., Douzou, P. & Sligar, S. G. (1992). Heme-pocket-hydration change during the inactivation of cyctochrome P-$450_{camphor}$ by hydrodtatic pressure. *Eur. J. Biochem*., *209*, 583–588.

[22] Ogliaro, F., de Visser, S. P. & Shaik, S. (2002). The 'push' effect of the thiolate ligand in cytochrome P450: a theoretical gauging. *J. Inorg. Biochem.*, *91*, 554–567.

[23] Rydberg, P., Sigfridsson, E. & Ryde, U. (2004). On the role of the axial ligand in heme proteins: a theoretical study. *J. Biol. Inorg. Chem.*, *9*, 203–223.

[24] Altun, A. & Thiel, W. (2005). Combined quantum mechanical/molecular mechanical study on the pentacoordinated ferric and ferrous cytochrome $P450_{cam}$ complexes. *J. Phys. Chem. B*, *109*, 1268–1280.

[25] Fantuzzi, A., Fairhead, M. & Gilardi, G. (2004). Direct electrochemistry of immobilized human cytochrome P450 2E1. *J. Am. Chem. Soc.*, *126*, 5040–5041.

[26] Sharrock, M., Debrunner, P. G., Schulz, C., Lipscomb, J. D., Marshall, V. & Gunsalus, I. C. (1976). *Biochim. Biophys. Acta*, *420*, 8–26.

[27] Champion, P. M., Lipscomb, J. D., Münck, E., Debrunner, P. & Gunsalus, I. C. (1975). Mossbauer investigations of high-spin ferrous heme proteins. I. Cytochrome P-450. *Biochemistry*, *14*, 4151–4158.

[28] Chottard, G., Schappacher, M., Ricard, L. & Weiss, R. (1984). Resonance Raman spectra of iron(II) cytochrome P450 model complexes: influence of the thiolate ligand. *Inorg. Chem*., *23*, 4557–4561.

[29] Bangcharoenpaurpong, O., Rizos, A. K., Champion, P. M., Jollie, D. & Sligar, S. G. (1986). Resonance raman detection of bound dioxygen in cytochrome P-450cam. *J. Biol. Chem.*, *261*, 8089–8092.

[30] Aikens, J. & Sligar, S. G. (1994). Kinetic solvent isotope effects during activation by cytochrome P-450cam. *J. Am. Chem. Soc.*, *116*, 1143–1144.

[31] Chance, B (1949). The primary and secondary compounds of catalase and methyl or ethyl hydrogen peroxide: II. Kinetics and activity, *J. Biol. Chem. 1949, 179,* 1341-1369.

[32] Kellner, D. G., Hung, S.-C., Weiss, K.E., & Sligar, S. G. Kinetic characterization of compound I formation in the thermostable cytochrome P450 CYP119, *J. Biol. Chem. 277,* 9641-9644.

[33] Kamachi, T. & Yoshizawa, K. (2003). A theoretical study on the mechanism of camphor hydroxylation by compound I of cytochrome P450. *J. Am. Chem. Soc.*, *125*, 4652–4661.

[34] Guallar, V. & Friesner, R. A. (2004). Cytochrome P450CAM enzymatic catalysis cycle: A quantum mechanics/molecular mechanics study. *J. Am. Chem. Soc.*, *126*, 8501–8508.

[35] Kumar, D., Hirao, H., de Visser, S. P., Zheng, J., Wang, D., Thiel, W. & Shaik, S. (2005) New features in the catalytic cycle of cytochrome P450 during the formation of compound I from compound 0. *J. Phys. Chem. B*, *109*, 19946–19951.

[36] Newcomb, M., Aebisher, D., Shen, R., Chandrasena, R. E. P., Hollenberg, P. F. & Coon, M. J. (2003). Kinetic isotope effects implicate two electrophilic oxidants in cytochrome P450-catalyzed hydroxylations. *J. Am. Chem. Soc.*, *125*, 6064–6065.

[37] Davydov, R., Makris, T. M., Kofman, V., Werst, D. E., Sligar, S. G. & Hoffman, B. M.(2001). Hydroxylation of camphor by reduced oxy-cytochrome P450cam: Mechanistic implications of EPR and ENDOR studies of catalytic intermediates in native and mutant enzymes. *J. Am. Chem. Soc.*, *123*, 1403–1415.

[38] Kellner, D. G., Hung, S.-C., Weiss, K. E. & Sligar, S. G. (2002). Kinetic characterization of compound I formation in the thermostable cytochrome P450 CYP119. *J. Biol. Chem.*, *277*, 9641–9644.

[39] Denisov, I. G., Makris, T. M. & Sligar, S. G. (2001). Cryotrapped reaction intermediates of cytochrome P450 studies by radiolytic reduction with phosphorus-32. *J. Biol. Chem.*, *276*, 11648–11652.

[40] Hishiki, T., Shimada, H., Nagano, S., Egawa, T., Kanamori, Y., Makino, R., Park, S.-Y., Adachi, S.-I., Shiro, Y. & Ishimiura, Y. (2000). X-ray crystal structure and catalytic properties of Thr252Ile mutant of cytochrome P450cam: Roles of Thr252 and water in the active center. *J. Biochem.*, *128*, 965–974.

[41] Schlichting, I., Berendzen, J., Chu, K., Stock, A. M., Maves, S. A., Benson, D. E., Sweet, R. M., Ringe, D., Petsko, G. A. & Sligar, S. G. (2000). The catalytic pathway of cytochrome P450cam at atomic resolution. *Science*, *287*, 1615–1622.

[42] Groves, J. T. & McClusky, G. A. (1976). Aliphatic hydroxylation via oxygen rebound. Oxygen transfer catalyzed by iron. *J. Am. Chem. Soc.*, *98*, 859–861.

[43] Ogliaro, F., Harris, N., Cohen, S., Filatov, M., de Visser, S. P. & Shaik, S. (2000). A model "rebound" mechanism of hydroxylation by cytochrome P450: Stepwise and effectively concerted pathways, and their reactivity patterns. *J. Am. Chem. Soc.*, *122*, 8977–8989.

[44] de Visser, S. P., Kumar, D., Cohen, S., Shacham, R. & Shaik, S. (2004). A predictive pattern of computed barriers for C-H hydroxylation by compound I of cytochrome P450. *J. Am. Chem. Soc.*, *126*, 8362–8363.

[45] Yoshizawa, K., Kamachi, T. & Shiota, Y. (2001). A theoretical study of the dynamic behavior of alkane hydroxylation by a compound I model of cytochrome P450. *J. Am. Chem. Soc.*, *123*, 9806–9816.

[46] Wang,Q., Sheng, X., Horner, J. H., & Newcomb, M. (2009). Quantitative Production of Compound I from a Cytochrome P450 Enzyme at Low Temperatures. Kinetics, Activation Parameters, and Kinetic Isotope Effects for Oxidation of Benzyl Alcohol, *J. Am. Chem. Soc. 131*, 10629–10636.

[47] Newcomb, M., Zhang, R., Chandrasena, R. E. P., Halgrimson, J. A., Horner, J. H., Makris, T. M. & Sligar, S. G. (2006). Cytochrome P450 compound I. *J. Am. Chem. Soc.*, *128*, 4580–4581.

[48] Daiber, A., Herold, S., Schöneich, C., Namgaladze, D., Peterson, J. A. & Ullrich, V. (2000). Nitration and inactivation of cytochrome P450BM-3 by peroxynitrite. *Eur. J. Biochem.*, 267, 6729–6739.

[49] Newcomb, M., Halgrimson, J. A., Horner, J. H., Wasinger, E. C., Chen, L. X. & Sliger, S. G. (2008). X-ray absorption spectroscopic characterization of a cytochrome P450 compound II derivative. *Proc. Natl. Acad. Sci. USA*, *105*, 8179–8184.

[50] Hamberg, M. & Samuelsson, B. (1974). Prostaglandin Endoperoxides. Novel transformations of arachidonic acid in human platelets. *Proc. Natl. Acad. Sci. USA, 71*, 3400–3404.

[51] Hamberg, M., Svensson, J. & Samuelsson, B. (1974). Prostaglandin endoperoxides. A new concept concerning the mode of action and release of prostaglandins. *Proc. Natl. Acad. Sci. USA, 71*, 3824–3828.

[52] Hamberg, M., Svensson, J. & Samuelsson, B. (1975). Thromboxanes: A new group of biologically active compounds derived from prostaglandin endoperoxides, *Proc. Natl. Acad. Sci. USA*, *72*, 2994 – 2998

[53] Herz, W., Ligon, R. C. Turner, J. A. & Blount, J. F. (1977). Remote oxidation in the Fe(II)-induced decomposition of a rigid epidioxide. *J. Org. Chem.*, *42*, 1885-1895.

[54] Turner, J. A. & Herz, W. (1977). Iron(II)-induced decomposition of epidioxides derived from α-phellandrene. *J. Org. Chem.*, *42*, 1895-1900.

[55] Turner, J. A. & Herz, W. (1977). Iron(II)-induced decomposition of unsaturated cyclic peroxides derived from butadienes. A simple procedure for synthesis of 3-alkylfurans. *J. Org. Chem.*, *42*, 1900-1904.

[56] Turner, J. A. & Herz, W. (1977). Fe(II)-induced decomposition of epidioxides. A chemical model for prostaglandin E, prostacyclin and thromboxane biosynthesis. *Experientia*, *33*, 1133–1134.

[57] Diczfalusy, U., Falardeau, P. & Hammarström, S. (1977). Conversion of prostaglandin endoperoxides to C_{17}-hydroxy acids catalyzed by human platelet thromboxane synthase. *FEBS Lett*., *84*, 271–274.

[58] Diczfalusy, U. & Hammarström, S. (1980). Biosynthesis of thromboxanes. *Adv. Prostaglandin Thromboxane Res., 6*, 267–274.

[59] Fried, J. & Barton, J. (1977). Synthesis of 13,14-dehydroprostacyclin methyl ester: A potent inhibitor of platelet aggregation. *Proc. Natl. Acad. Sci. USA*, *74*, 2199–2203.

[60] [Graf, H. Ruf, H. H. & Ullrich, V. (1983). Prostacyclin synthase, a cytochrome P450 enzyme. *Angew. Chem. Int. Ed. Engl*., *22*, 487–488.

[61] [Haurand, M, & Ullrich, V. (1985). Isolation and characterization of thromboxane synthase from human platelets as a cytochrome P-450 enzymes. *J. Biol. Chem.*, *260*, 15059–15067.

[62] Hsu, P.-Y., Tsai, A.-L., Kulmacz, R. J. & Wang, L.-H. (1999). Expression, purification, and spectroscopic characterization of human thromboxane synthase. *J. Biol. Chem*, *274*, 762–769.

[63] Ullrich, V. & Brugger, R. (1994). Prostacyclin and thromboxane synthase: New aspects of hemethiolate catalysis. *Angew. Chem. Int. Ed. Engl.*, *33*, 1911–1919.

[64] Hecker, M. & Ullrich, V. (1989). On the mechanism of prostacyclin and thromboxane A_2 biosynthesis. *J. Biol. Chem*., *264*, 141–150.

[65] Chen, Z., Wang, L.-H. & Schelvis, J. P. M. (2003). Resonance Raman investigation of the interaction of thromboxane synthase with substrate analogues. *Biochemistry*, *42*, 2542–2551.

[66] Hsu, P.-Y., Tsai, A.-L., Kulmacz, R. J. & Wang, L.-H. (1999). Expression, purification, and spectroscopic characterization of human thromboxane synthase. *J. Biol. Chem*, *274*, 762–769.

[67] Dawson, J. H., Andersson, L. A. & Sono, M. (1982). Spectroscopic investigations of ferric cytochrome P-450-CAM ligand complexes: Identification of the ligand trans to cysteinate in the native enzyme. *J. Biol. Chem.*, *257*, 3606–3617.

[68] Yeh, H.-C., Hsu, P.-Y., Wang, J.-S., Tsai, A.-L. & Wang, L.-H. (2005). Characterization of heme environment and mechanism of peroxide bond cleavage in human prostacyclin synthase. *Biochim. Biophys. Acta*, *1738*, 121–132.

[69] Yeh, H.-C., Tsai, A.-L. & Wang, L.-H. (2007). Reaction mechanisms of 15-hydroperoxyeicosatetraenoic acid catalyzed by human prostacyclin and thromboxane synthases. *Arch. Biochem. Biophys.*, *461*, 159–168.

[70] Yamane, T., Makino, K., Umezawa, N., Kato, N. & Higuchi, T. (2008). Extreme rate acceleration by axial thiolate coordination on the isomerization of endoperoxide catalyzed by iron porphyrin. *Angew. Chem. Int. Ed. Engl.*, *47*, 6438-6440.

[71] [Wang, L.-H., Tsai, A.-L. & Hsu, P.-Y. (2001). Substrate binding is the rate limiting step in thromboxane synthase catalysis. *J. Biol. Chem.*, *276*, 14737–14743.

[72] [Nüsing, R., Schneider-Voss, S. & Ullrich, V. (1990). Immunoaffinity purification of thromboxane synthase. *Arch. Biochem. Biophys.*, *3*, 175-180.

[73] Yokoyama, C., Miyata, A., Ihara, H., Ullrich, V. & Tanabe, T. (1991) Molecular cloning of human platelet thromboxane A synthase. *Biochem. Biophys. Res. Commun*., *178*, 1479-1484.

[74] Ohashi, K., Ruan, K.-H., Kulmacz, R. J., Wu, K. K. & Wang, L.-H. (1992) Primary structure of thromboxane synthase determined from the cDNA sequence. *J. Biol. Chem*., *267*, 787-793.

[75] Tone, Y., Miyata, A., Hara, S., Yukawa, S. & Tanabe, T. (1994). Abundant expression of thromboxane synthase in rat macrophages. *FEBS Lett*., *340*, 241-244.

[76] Zhang, L., Chase, M. B. & Shen, R. F. (1993). Molecular cloning and expression of murine thromboxane synthase. *Biochem. Biophys. Res. Commun.*, *194*, 741-748.

[77] Shen, R.-F., Zhang, L., Baek, S. J., Tai, H.-H. & Lee, K.-D. (1994). The porcine thromboxane synthase-encoding cDNA: sequence, mRNA expression and enzyme production in Sf9 insect cells. *Gene*, 140, 261-265.

[78] Xia, Z, Shen, R.-F., Baek, S. J. & Tai, H.-H. (1993). Expression of two different forms of cDNA for thromboxane synthase in insect cells and site-directed mutagenesis of a critical systeine residue. *Biochem. J.*, *295*, 457–461.

[79] Ruan, K.-H., Milfeld, K., Kulmacz, R. J. & Wu, K. K. (1994). Comparison of the construction of a 3-D model for human thromboxane synthase using P450cam and BM-3 as templates: Implications for the substrate binding pocket. *Protein Eng.*, *7*, 1345–1351.

[80] Wang, L.-H., Matijevic-Aleksic, N., Hsu, P.-Y., Ruan, K.-H., Wu, K. K. & Kulmacz, R. J. (1996). Identification of thromboxane A_2 synthase active site residues by molecular modeling-guided site-directed mutagenesis. *J. Biol. Chem.*, *271*, 19970–19975.

[81] Hsu, P.-Y., Tsai, A.-L. & Wang, L.-H. (2000). Identification of thromboxane synthase amino acid residues involved in heme-propionate binding. *Arch. Biochem. Biophys.*, *383*, 119–127.

[82] Inoue. M., Smith, W.L. & Dewitt, D. L. (1987). Molecular characterization of the prostacyclin synthase. *Adv. Prostaglandin Thromboxane Leukot. Res.*, *17*, 29-33.

[83] Hara, S., Miyata, A., Yokoyama, C., Inoue, H., Brugger, R., Lottspeich, F., Ullrich, V. & Tanabe, T. (1994). Isolation and molecular cloning of prostacyclin synthase from bovine endothelial cells. *J. Biol. Chem*., *269*, 19897-19903.

[84] Miyata, A., Hara, S., Yokoyama, C., Inoue, H., Ullrich, V. & Tanabe, T. (1994) Molecular cloning of human prostacyclin synthase. *Biochem. Biophys. Res. Commun.*, *200*, 1728-1734.

[85] Tone, Y., Inoue, H., Hara, S., Yokoyama, C., Hatae, T., Oida, H., Narumiya, S., Shigemoto, R., Yukawa, S., and Tanabe, T. (1997) The regional distribution and cellular localization of mRNA encoding rat prostacyclin synthase. *Eur. J. Cell Biol.* **72**, 268–277.

[86] Kuwamoto, S., Inoue, H., Tone, Y., Izumi, Y., and Tanabe, T.(1997) Inverse gene expression of prostacyclin and thromboxane synthases in resident and activated peritoneal macrophages. *FEBS Lett.* 409, 242–246.

[87] Li, Y.-C., Chiang, C.-W., Yeh, H.-C., Hsu, P.-Y., Whitby, F. G., Wang, L.-H. & Chan, N.-L. (2008). Structure of prostacyclin synthase and its complexes with substrate analog and inhibitor reveal a ligand-specific heme conformation change. *J. Biol. Chem*., *283*, 2917–2926.

[88] Hatae, T., Hara, S., Yokoyaman, C., Yabuki, T., Inoue, H., Ullrich, V. & Tanabe, T. (1996). Site-directed mutagenesis of human prostacyclin synthase: Alternation of Cys^{441} of the Cys-pocket, and Glu^{347} and Arg^{350} of the EXXR motif. *FEBS lett*., *389*, 268-272.

[89] Shyue, S.-K., Ruan, K.-H., Wang, L.-H. & Wu, K. K. (1997). Prostacyclin synthase active site. *J. Biol. Chem.*, *272*, 3657-3662.

[90] Chiang, C.-W., Yeh, H.-C., Wang, L.-H. & Chan, N.-L. (2006). Crystal structure of the human prostacyclin synthase. *J.Mol.Biol., 364*, 266–274.

[91] Ruan, K.-H., Wu, J. & Cervantes, V. (2008). Characterization of the substrate mimic bound to engineered prostacyclin synthase in solution using high-resolution NMR spectroscopy and mutagenesis: Implication of the molecular mechanism in biosynthesis of prostacyclin. *Biochemistry*, *47*, 680–688.

[92] Becke, A. D. (1993). Density-functional thermochemistry. III. The role of exact exchange. *J. Chem. Phys.*, *98*, 5648–5652

[93] Lee, C., Yang, W. & Parr, R. G. (1988). Development of the Colle-Salvetti correlation-energy formula into a functional of the electron density. *Phys. Rev. B*, *37*, 785–789.

[94] Yanai, T. K. & Mori, S. (2008). Density functional studies on thromboxane biosynthesis: Mechanism and role of the heme-thiolate system. *Chem. Asian J.*, *3*, 1900–1911.

[95] Yanai, T. K. & Mori, S. (2009). Density functional studies on isomerization of prostaglandin H_2 to prostacyclin catalyzed by cytochrome P450. *Chem. Eur. J.*, *15*, 4464-4473.

[96] Wang, Y., Chen, H., Makino, M., Shiro, Y., Nagano, S., Asamizu, S., Onaka, H. & Shaik, S. (2009). Theoretical and experimental studies of the conversion of chromopyrrolic acid to an antitumor derivative by cytochrome P450 StaP: The catalytic role of water molecules. *J. Am. Chem. Soc*., *131*, 6748–6762.

[97] Wang, Y., Hirao, H., Chen, H., Onaka, H., Nagano, S. & Shaik, S. (2008). Electron transfer activation of chromopyrrolic acid by cytochrome P450 en route to the formation of an antitumor indolocarbazole derivative: Theory supports experiment. *J. Am. Chem. Soc.*, *130*, 7170–7171.

[98] Urade, Y., Tanaka, T., Eguchi, N., Kikuchi, M., Kimura, H., Toh, H. & Hayaishi, O. (1995). Structural and Functional Significance of Cysteine Residues of Glutathione-independent Prostaglandin D Synthase, *J. Biol. Chem. 270*, 1422-1428.

[99] Kumasaka, T., Aritake, K., Ago, H., Irikura, D., Tsurumura, T.,Yamamoto, M., Miyano, M., Urade, Y., & Hayaishi, O. (2009). Structural Basis of the Catalytic Mechanism Operating in Open-Closed Conformers of Lipocalin Type Prostaglandin D Synthase, *J. Biol. Chem. 284*, 22344–22352

[100] Uchida, Y., Urade, Y., Mori, S. & Kohzuma, T. (2010). UV resonance Raman studies on the activation mechanism of human hematopoietic prostaglandin D_2 synthase by a divalent cation, Mg^{2+}, *J. Inorg. Biochem.,* in press.

[101] Yamada, T., Komoto, J., Watanabe, K., Omiya., Y., & Takusagawa, F. (2005). Crystal Structure and Possible Catalytic Mechanism of Microsomal Prostaglandin E Synthase Type 2 (mPGES-2). *J. Mol. Biol. 348*, 1163–1176.